Available online at www.sciencedirect.com

SciVerse ScienceDirect

Physics Procedia 32 (2012) 914 – 919

Physics Procedia

The Effect of Nitrided Layer on Antibacterial properties for Biomedical Stainless Steel

C. F. Hung[a,b], C. Z. Wu[a], W. F. Lee[a], K. L. Ou[c,d,e**], C. M. Liu[c,f,g], P. W. Peng[c,d,h,*]

[a]*School of Dentistry, Taipei Medical University, Taipei 110,Taiwan*
[b]*Department of Dentistry, Taipei Medical University Hospital, Taipei 110, Taiwan*
[c]*Research Center for Biomedical Implants and Microsurgery Devices, Taipei Medical University, Taipei 110, Taiwan*
[d]*Research Center for Biomedical Devices, Taipei Medical University, Taipei 110, Taiwan*
[e]*Graduate Institute of Biomedical Materials and Engineering, Taipei Medical University, Taipei 110, Taiwan*
[f]*Department of Chemical and Material Engineering, LungHwa University of Science and Technology, Taoyuan 306, Taiwan*
[g]*Graduate School of Engineering Technology, LungHwa University of Science and Technology, Taoyuan 306, Taiwan*
[h]*School of Dental Technology, Taipei Medical University, Taipei 110, Taiwan*

Abstract

Plasma nitriding of AISI type 303 austenitic stainless steel using microwave system at various input powers was conducted in present study. The nitrided layers were characterized via scanning electron microscopy, transmission electron microscopy and Vickers microhardness tester. The anti-bacterial property of this nitrided layer was also evaluated. The analytical results revealed the hardness of AISI type 303 stainless steel could be enhanced with nitriding process. The microstructure of the nitrided layer comprised of nitrogen-expanded γ phase. Bacterial test demonstrated the nitrided layer processed the excellent anti-bacterial properties. The enhanced hardness and anti-bacterial properties make the nitrided AISI type 303 austenitic stainless steel the potential material in the biomedical applications.

PACS: Type pacs here, separated by semicolons ;

Keywords: austenitic stainless steel; microwave plasma; nitriding; anti-bacterial property

1. Introduction

While American Iron and Steel Institute (AISI) type 304 and 316 austenitic stainless steels (ASSs) are used in a wide range of biomedical applications in orthopaedics and dentistry, higher work-hardening rate and toughness are the main drawbacks to reduce the machinability and to increase the cost. From the perspectives of economic and manufacturing, free-machining stainless steel, such as 303 grade with an addition of sulfur content, is an attractive alternative to reduce machining process and to improve surface quality [1]. Compared with type 316, AISI type 303 has higher yield strength and requires greater stress to permanently deform, making it suitable for orthodontic brackets [2]. However, relatively lesser resistant to the corrosion is still controversial [3, 4].

The orthodontic bracket is an intermedia, which transfers the exact force from the wire to teeth, leading to the tooth movement. Materials with strong resistances to fracture and deformation were essential requirements for

* Corresponding author. ** Co-corresponding author. Tel.: 886-2-27361661 ext.5140
E-mail address:apon@tmu.edu.tw.

1875-3892 © 2012 Published by Elsevier B.V. Selection and/or peer review under responsibility of Chinese Vacuum Society (CVS).
Open access under CC BY-NC-ND license. doi:10.1016/j.phpro.2012.03.656

orthodontic applications. In the oral cavity, the severe physical conditions, such as the presence of dental plaque or a high chloride ion concentration, hasten the corrosion rate of orthodontic bracket [2]. Meanwhile, a large amount of bacterial adhesion and plaque formation usually result in the infections and immune responses. It is well documented that the interactions between protein adsorption and the metal bracket are mostly determined by chemical and physical properties of metal surface [5]. Hence, the improvement in bioreaction on the implant surface could be obtained by creating multifunctional surface with several surface modifications [5-11].

Plasma nitriding is a thermochemical treatment associated with nitrogen incorporation into the bulk material [12]. Notably, plasma-assisted nitriding at temperature below 500 ℃ improves not only the surface hardness, but also the corrosion resistance by producing the metastable FCC composed of supersaturated nitrogen atoms in the SS matrix [13-15]. It is well known that nitrogen is a beneficial austenite-stabilizing element, which efficiently intensifies the resistance to localized corrosion [16].

There are very few studies of AISI type 303 for biomedical applications to date. In order to make sure that AISI type 303 is a potential material for orthodontic brackets, plasma nitriding was applied to enhance the mechanical properties, especially those related to the surface hardness and corrosion resistance. The influences of plasma nitriding on mechanical properties of AISI 303 stainless steel were covered, including electrical measurements and material analyses. We also examined the effects on *in vitro* the antibacterial measurements with JIS Z2801:2000 specification [17], in comparison with 304 SS.

2. Experimental

The material investigated in the present study was AISI 303 austenite stainless steel (Hung-Chun Bio-S Co., Ltd.) with the composition (wt. %): C, <0.15; Si, <1.0; Mn, <2.0; Cr, 17.0~19.0; Ni, 8.0~10.0; P, <0.02; S, >0.15; and Fe, balance. The specimens were cut from 16 mm diameter bars with a thickness of 1.5 mm. All substrates were applied to a mechanical polishing, a combination of SiC paper grinding to 4000 grit and Al_2O_3 solution polishing to 1 μm. Prior to being loaded into the heated holder, the specimens had been cleaned with acetone in an ultrasonic bath for 10 minutes followed by air drying.

AISI 303 SS specimens were nitrided by microwave plasma assisted system (AST-MW1200W) under a gas mixture composed of 40 % N_2 and 60 % H_2. Plasma was generated in a quartz tube by the frequency of 2.45 GHz with various input powers ranging from 300 to 800 W. The nitriding treatments were performed at 450 ^oC for 60 min under the pressure of 4 Torr.

Scanning electron microscopy (SEM, JSM-6500, Japan) was employed to observe the morphologies of the treated specimens. The elemental concentration depth profiles were measured by SEM equipped with an energy dispersive spectrometer (EDS, INCA Wave, UK). The microstructures of the treated specimens were characterized by X-ray diffraction (XRD, Kegaku2000, Japan) and high-resolution transmission electron microscopy (HRTEM, JEOL-80, Japan). The hardness of nitrided layer was measured by a Vickers microhardness tester (FM-100e, Japan).

Escherichia coli (*E. coli,* ATCC8739) was used for bacterial test with nitrided layers to determine the antibacterial activity using according to Japanese Industrial Standard (JIS) No. Z2801:2000. A single colony of the strain was first streaked from a frozen stock with streak plate method on nutrition agar plates. Before bacterial inoculation the suspension was diluted by nutrition broth to a density of 4×10^5 CFU/ml and then dropped onto specimens for incubation at 37 °C / 95 % humidity for a period of 24 h.

The harvested bacterial suspension was underwent a series of dilutions by PBS to yield a concentration of 10^1, 10^2, 10^3 and 10^4 fold, respectively. The diluted suspension was then inoculated onto nutrition agar plate and cultured at 37 °C for 24 h. The number of bacterial colonies was counted to obtain the number of bacteria adhered on the plate. The antibacterial activity calculated by equation (1) was recognized the antibacterial effect.

$$\text{Antibacterial rate (AR)} = 100 \times (N_2 - N_1) / N_2\ (\%) \qquad (1)$$

N_1: number of bacteria adhered on the tested sample after 24 hours incubation

N_2: number of bacteria adhered on the control group after 24 hours incubation

3. Results and Discussions

Fig. 1 showed the depth penetration of nitrogen at various input power using EDX measurements. As can be seen, with the power of 700W, the nitrogen penetration was proportional to the input power and reached the maximum

amount of 29 at.%. Increasing the input power boosted up the kinetic energy of nitrogen ions and, in turn, enhanced nitrogen penetration [18]. Particularly, the nitrogen content with the power of 800W was lower than that of 700 W. It could be deduced that the diffusion rate of nitrogen atom was faster than recombination rate with higher excitation energy. Threshold energy of 800 W was in favor of the N-atom recombination to form nitrogen molecules, competed with the N-atom diffusion into the substrate resulting in the formation of the nitrided layer [14].

Compared with the substrate, the nitrided layer which had a better corrosion resistance to the same acid etchant was apparently observed. The consistent nitrided layer without precipitation was presented in the cross-sectional SEM images of Fig. 2. In conformity with the results of the depth penetration of nitrogen atoms, the maximum thickness of 5.625 μm was reached with the input power of 700W. The penetration of nitrogen atoms mastered the thickness of the nitrided layer based on the positive correlation between the growth kinetics of the nitrided layer and the depth profiles of nitrogen [19]. It was expected that the thicker nitrided layer was obtained as the input power increased.

The structures of nitrided layers as a function of excitation energy were investigated using XRD as shown in Fig. 3. According to the patterns, the substrate consisted of the peaks corresponding to a set of austenitic face-centered-cubic (FCC) γ phases. After nitriding, the peaks belonged to expanded austenite, which was denoted as γ_N phase, emerged, whereas γ phases disappeared due to the thicker nitrided layer. γ_N phase was attributed to a near FCC structure with a supersaturated solid solution of nitrogen in γ matrix without the nitride formation [20-22]. With an increase in power, the broadened peaks became more intensive and shifted towards 2θ angles lower, suggesting an energy-dependent behavior. These chiefly resulted from possible internal stresses and defect structures of γ_N-phase layer induced by the nitrogen incorporated [15, 23, 24]. In addition, the expanded lattice of the γ_N-phase layer induced by the insertion of nitrogen atoms as function of the excitation energy could be demonstrated by the calculation of Braggs Law. However, the estimated lattice parameter of a specimen nitrided at 800 W was similar with that at 700 W. The observation that the lattice rotation at the surface of the grains was reached the maximum at 700 W in good agreement with the results of the depth penetration of nitrogen. The results revealed the lattice variation was related with the content of nitrogen penetration [25]. From the observations above, the main influences of the excitation energy on microstructure were the nitrogen penetration and the depth of γ_N-phase layer, instead of the phase transformation.

The variation of microhardness versus excitation energy of plasma nitriding was illustrated in Fig. 4. As shown, the microhardness of γ_N-phase layer increased when the input power increased. The value of microhardness under a load of 10 g increased from 176 HV for a substrate up to 1486 HV with an input power of 700 W, which could be increased by approximately a factor of 8 compared with the substrate. It could be inferred the raise of γ_N-phase layer thickness and high nitrogen contents in this layer increased in the microhardness of the corresponding layer. The significantly high microhardness could be explained by large compressive residual stresses and reticular distortions in the high enriched γ_N-phase layer [21, 26, 27]. As a matter of fact, a higher expanded lattice obtained from the XRD analysis at higher input power (no larger than 700 W) reasonably demonstrated the higher microhardness of γ_N-phase layer. Lately, the high microhardness of γ_N-phase layer study has been closer to other research work and other hard thin films, such as TiO_2, TiN and the diamond-like films we studied before [28]. As stated above, the hardness of γ_N-phase layer was far from the substrate effects and enhanced the biomedical applications in the severe body fluids.

The antibacterial test against *E. coli* of AISI type 303 SS with and without nitrided layer were carried out in comparison with type 304. It revealed the untreated sample whether 303 or 304 did not possess any antibacterial property. By contrast, the AR ratio approached to 99 % as the stainless steel which treated by plasma nitriding. It was indicate that the nitrided layers exhibited excellent ability to inhibit the growth of *E. coli*. However, for applications in biomedical materials further experiments are required to investigate the interaction between tissues and nitrided layer formed on AISI type 303 SS.

4. Conclusion

The microstructure and composition of nitrided layers on AISI type 303 produced using microwave plasma as function of the input powers. The lattice expansions of nitrided layers from γ phase to γ_N phase were occurred. The thickness and hardness of the nitrided layer were positive correlation with input power.

5. Acknowledgements

The authors highly appreciated Wen-Li Zeng for participation in experiments. We highly acknowledge financial support of research by Center of Excellence for Clinical Trial and Research in Neurology and Neurosurgery, Taipei Medical University-Wan Fang Hospital under the grand number of DOH99-TD-B-111-003.

6. References

[1] W. Liang, Appl Surf Sci 211 (2003) 308.
[2] K.T. Oh, S.U. Choo, K.M. Kim, K.N. Kim, Eur J Orthod 27 (2005) 237.
[3] M. Pisarek, P. Kędzierzawski, M. Janik-Czachor, K. Kurzydłowski, J Solid State Chem 13 (2009) 283.
[4] R. Matos de Souza, L. Macedo de Menezes, Angle Orthod 78 (2008) 345.
[5] H.C. Cheng, S.Y. Chiou, C.M. Liu, M.H. Lin, C.C. Chen, K.L. Ou, J Alloy Compd 477 (2009) 931.
[6] K.L. Ou, C.T. Lin, S.L. Chen, C.F. Huang, H.C. Cheng, Y.M. Yeh, K.H. Lin, J Electrochem Soc 155 (2008) E79.
[7] K.L. Ou, J. Wu, W.F.T. Lai, C.B. Yang, W.C. Lo, L.H. Chiu, J. Bowley, J Biomed Mater Res B 92A (2010) 906.
[8] C. F. Huang, H. C. Cheng, C. M. Liu, C. C. Chen, K.-L. Ou, J Vac Sci Technol B 476 (2009) 683.
[9] H.C. Cheng, S.Y. Lee, C.C. Chen, Y.C. Shyng, K.L. Ou, J Electrochem Soc 154 (2007) E13.
[10] Y.H. Shih, C.T. Lin, C.M. Liu, C.C. Chen, C.S. Chen, K.L. Ou, Appl Surf Sci 253 (2007) 3678.
[11] K.L. Ou, Y.H. Shih, C.F. Huang, C.C. Chen, C.M. Liu, Appl Surf Sci 255 (2008) 2046.
[12] F. Cemin, F.G. Echeverrigaray, A.C. Rovani, C.L.G. Amorim, R.L.O. Basso, I.J.R. Baumvol, C.A. Figueroa, Mat Sci Eng A 527 (2010) 3206.
[13] M.P. Fewell, D.R.G. Mitchell, J.M. Priest, K.T. Short, G.A. Collins, Surf Coat Technol 131 (2000) 300.
[14] N. Renevier, P. Collignon, H. Michel, T. Czerwiec, Surf Coat Technol 111 (1999) 128.
[15] J. Wang, J. Xiong, Q. Peng, H. Fan, Y. Wang, G. Li, B. Shen, Mater Charact 60 (2009) 197.
[16] P. Wan, Y. Ren, B. Zhang, K. Yang, Mat Sci Eng C In Press, Corrected Proof (2010).
[17] K.H. Liao, K.L. Ou, H.C. Cheng, C.T. Lin, P.W. Peng, Appl Surf Sci In Press, Corrected Proof (2010).
[18] J.H. Liang, C.S. Wang, W.F. Tsai, C.F. Ai, Surf Coat Technol 201 (2007) 6638.
[19] A. Saker, C. Leroy, H. Michel, C. Frantz, Mat Sci Eng A 140 (1991) 702.
[20] M.K. Lei, X.M. Zhu, Biomaterials 22 (2001) 641.
[21] A. Fossati, F. Borgioli, E. Galvanetto, T. Bacci, Surf Coat Technol 200 (2006) 3511.
[22] J.C. Stinville, P. Villechaise, C. Templier, J.P. Riviere, M. Drouet, Surf Coat Technol 204 (2009) 1947.
[23] L. Wang, S. Ji, J. Sun, Surf Coat Technol 200 (2006) 5067.
[24] M. Olzon-Dionysio, M. Campos, M. Kapp, S. de Souza, S.D. de Souza, Surf CoatTechnol 204 (2010) 3623.
[25] J.C. Stinville, P. Villechaise, C. Templier, J.P. Riviere, M. Drouet, Acta Mater 58 (2010) 2814.
[26] L. Shen, L. Wang, Y. Wang, C. Wang, Surf Coat Technol 204 (2010) 3222.
[27] T. Borowski, J. Jelenkowski, M. Psoda, T. Wierzchon, Surf Coat Technol 204 (2010) 1375.
[28] F.M. El-Hossary, N.Z. Negm, A.M.A. El-Rahman, M. Hammad, C. Templier, Surf Coat Technol 202 (2008) 1392.

Figure Captions

Fig. 1. The depth penetration of nitrogen at various input power
Fig. 2. Cross-sectional SEM images of nitrided layer
Fig. 3. XRD spectra of nitrided layers as a function of excitation energy
Fig. 4. The microhardness of nitrided layer with various input power
Fig. 5. The antibacterial properties of 303 SS with/without nitriding.

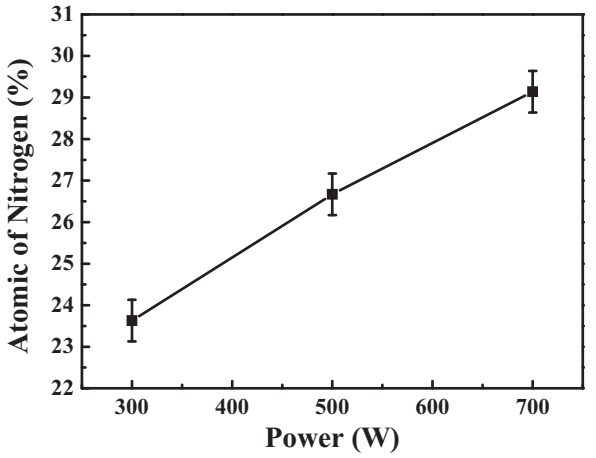

Fig. 1. K.L. Ou

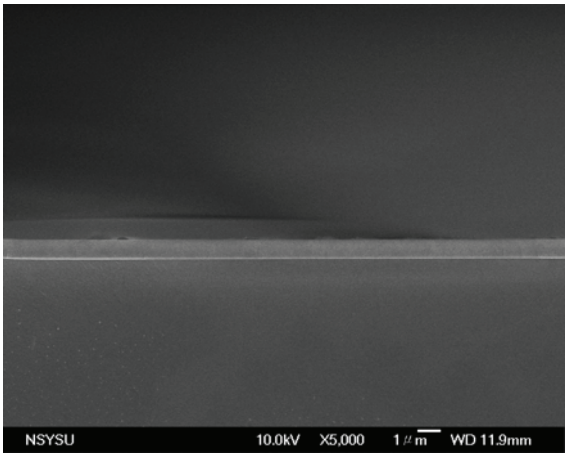

Fig. 2. K.L. Ou

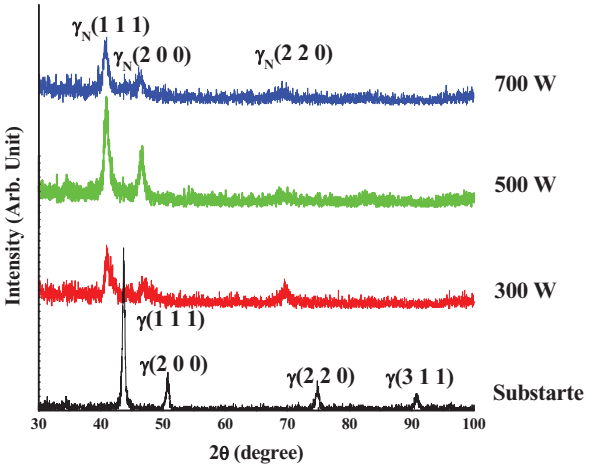

Fig. 3. K.L. Ou

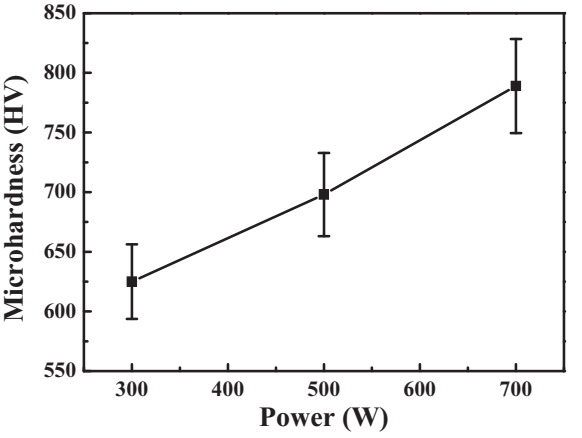

Fig. 4. K.L. Ou

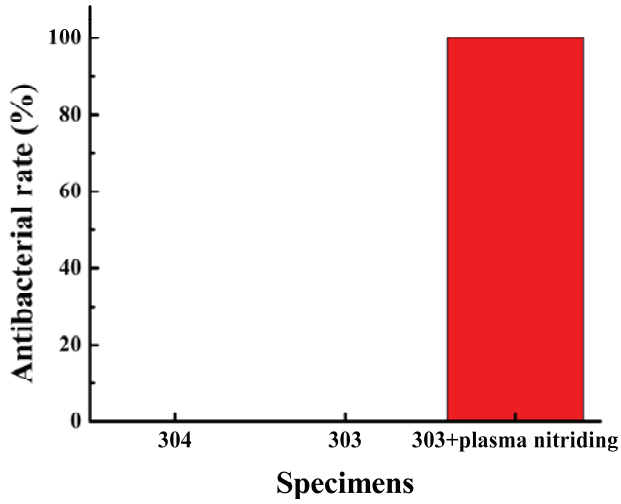
Antibacterial rate (%)
100
80
60
40
20
0
304
303
303+plasma nitriding
Specimens

Fig. 5. K.L. Ou